
Article:
Liu, F., Martins, L.M.P., Brash, A.J. et al. (2016) Ultrafast Depopulation of a Quantum Dot by LA-phonon-assisted Stimulated Emission. Physical Review B , 93. 161407(R. ISSN: 2469-9950

https://doi.org/10.1103/PhysRevB.93.161407

Ultrafast Depopulation of a Quantum Dot by LA-phonon-assisted Stimulated Emission

F. Liu,[1,*] L. M. P. Martins,[1] A. J. Brash,[1] A. M. Barth,[2] J. H. Quilter,[1,3] V. M. Axt,[2] M. S. Skolnick,[1] and A. M. Fox[1]

[1] *Department of Physics and Astronomy, University of Sheffield, Sheffield, S3 7RH, United Kingdom*
[2] *Institut für Theoretische Physik III, Universität Bayreuth, 95440 Bayreuth, Germany*
[3] *Department of Physics, Royal Holloway, University of London, Egham, TW20 0EX, United Kingdom*

We demonstrate ultrafast *incoherent* depopulation of a quantum dot from above to below the transparency point using LA-phonon-assisted emission stimulated by a red-shifted laser pulse. The QD is turned from a weakly vibronic system into a strongly vibronic one by laser driving which enables the phonon-assisted relaxation between the excitonic components of two dressed states. The depopulation is achieved within a laser pulse-width-limited time of 20 ps and exhibits a broad tuning range of a few meV. Our experimental results are well reproduced by path-integral calculations.

The exciton-phonon coupling in semiconductor quantum dots (QDs) has attracted much interest due to its importance both in fundamental physics and in semiconductor-based quantum technologies [1–4]. It has been known for some time that QDs can be excited by phonon-assisted transitions when the laser is detuned within the phonon sideband [5]. Very recently, it has been shown that population inversion can be achieved under these incoherent pumping conditions in the strong driving regime [6–13]. However, the opposite process in which an exciton in an inverted QD is de-excited with the assistance of longitudinal acoustic (LA) phonons has yet to be investigated. This process could be important for the development of tunable single QD lasers [14, 15] or of QD single-photon sources in cavities with improved timing jitter [1, 16, 18].

The significance of the LA phonon-assisted de-excitation process can be appreciated by comparing it to the conventional understanding of inverted 2-level systems. Consider a quantum dot in which population inversion has been created as shown in Fig. 1(a). A resonant laser pulse that is short compared to the spontaneous emission time, but long compared to the coherence time will only drive the system towards the transparency point, never crossing it due to the equal cross sections of stimulated emission and absorption [see Fig. 1(b)]. However, if the dot is coupled to the lattice, stimulated emission can be induced by a red-shifted pulse via phonon emission, provided that the temperature is low enough that phonon absorption is weak [see Fig. 1(c)]. The decoupling of stimulated emission and absorption enables depopulation of the inverted 2-level system to below the transparency point before spontaneous emission occurs, which is impossible for exactly resonant excitation in the incoherent limit. This process is fundamentally different to conventional vibronic systems - e.g. Ti:sapphire [19] - in that the phonon coupling is weak at low light intensities, and only becomes effective at high optical powers during a strong laser pulse. In this sense, the new mechanism can be regarded as de-excitation by *dynamic* vibronic coupling.

In this Rapid Communication, we demonstrate the LA-phonon-assisted stimulated emission (LAPSE) process by using a red-shifted laser pulse to *incoherently* de-excite an inverted quantum dot to below the transparency point. The time dynamics indicate that the depopulation occurs in 20 ps, limited by the laser pulse width. We show that the process occurs over a broad tuning range of $\sim$ 4 meV (in contrast to the fixed frequency of resonant excitation) and that the results are in a good agreement with path-integral calculations [20]. The new mechanism provides a route to ultrafast reset of an excited quantum dot, which should be important for quantum photonic systems incorporating dots as the nonlinear element.

Our experiments are performed on a device consisting of InGaAs QDs embedded in the intrinsic region of an $n-i-$Schottky diode. The sample is held at $T = 4.2$ K in a helium bath cryostat. The excitation laser pulse is derived by spectral shaping of the output from a mode-locked Ti:sapphire laser with repetition rate 76.2 MHz. The spectral FWHM is 0.2 meV for the π pulse in all measurements and 0.2 or 0.42 meV for the red-shifted laser pulse, corresponding to a Fourier transform limited pulse duration τ_{L} of 16.8 or 8 ps. τ_{L} is defined as the FWHM of the electric field envelope. The exciton population created by the circularly polarized laser pulse is determined by measuring the photocurrent (PC) generated when a reverse bias voltage is applied to the diode [21]. More details of the sample and experimental setup can be found in refs. 22–24.

A phenomenological description of the LAPSE process is as follows. Assume a QD is initially in the exciton state. A strong laser pulse red-shifted relative to the exciton state by $\hbar\Delta$ leads to the recombination of the exciton and the emission of a phonon and photon illustrated by thick down arrows in Fig. 1(c). To fully understand the underlying mechanism, we use the dressed state picture [see Fig. 1(d)]. In the rotating frame, the crystal ground state $|0\rangle$ and the incident laser field are treated as one state: $|0_{\mathrm{R}}\rangle$. The exciton state $|X\rangle$ and the laser field with one photon less are treated as $|X_{\mathrm{R}}\rangle$. The relative energies of the two states are shown by the

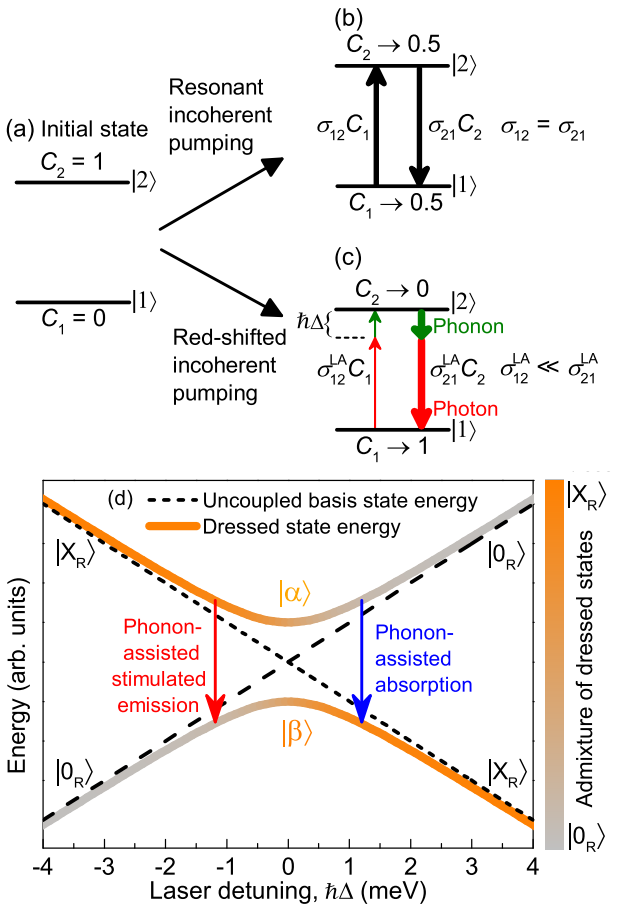

FIG. 1. (a-c): Difference between resonant incoherent pumping and red-shifted incoherent pumping. (a) A 2-level system is initially inverted ($C_2 > C_1$). C_i denotes the population of the i^{th} state. (b) Resonant incoherent pumping induces absorption and SE with equal cross sections ($\sigma_{12} = \sigma_{21}$), moving the system towards transparency ($C_1 = C_2$). σ denotes the absorption/stimulated emission cross section. (c) If pumped by red-shifted incoherent excitation, C_2 can be almost completely depleted as the red-shifted laser mainly induces SE ($\sigma_{12}^{\text{LA}} \ll \sigma_{21}^{\text{LA}}$). Absorption hardly occurs due to the lack of additional phonons at low temperature. (d) The mechanism of the LA-phonon-assisted SE and absorption explained in the dressed-state picture. $|0_{\text{R}}\rangle$, $|X_{\text{R}}\rangle$: uncoupled ground state and exciton state viewed in the rotating frame. $|\alpha\rangle$, $|\beta\rangle$: optically dressed states split by the effective Rabi energy $\hbar\Lambda$.

dashed/dotted lines in Fig. 1(d) as a function of the laser detuning $\hbar\Delta = \hbar(\omega_X - \omega_{\text{L}})$, where ω_X and ω_{L} are the angular frequencies of the exciton transition and laser, respectively. Since $|0_{\text{R}}\rangle$ and $|X_{\text{R}}\rangle$ are admixed by the laser field, the eigenstates of the system become two new optically dressed states: $|\alpha\rangle$ and $|\beta\rangle$, split by the effective Rabi energy $\hbar\Lambda(t) = \hbar\sqrt{\Delta^2 + \Omega(t)^2}$, where Ω is the Rabi frequency for resonant excitation proportional to the electric field amplitude E. The dressed state energies are shown by the thick solid lines in Fig. 1(d) and the color gradient illustrates the excitonic contribution to the corresponding states. Owing to their excitonic components, $|\alpha\rangle$ and $|\beta\rangle$ are coupled by LA-phonons via the deformation potential [25].

In the LAPSE process, the QD is initially in the $|X_{\text{R}}\rangle$ state. By applying a red-shifted laser pulse ($\Delta < 0$), the phonon-assisted relaxation channel is activated and the system relaxes from the higher-energy more exciton-like state $|\alpha\rangle$ to the lower-energy more ground-state-like state $|\beta\rangle$ by emitting phonons with an energy of $\hbar\Lambda$ [see red arrow in Fig. 1(d)]. If the phonon relaxation is fast enough, the system will reach thermal equilibrium between the two dressed states during the laser pulse. At low temperatures ($k_{\text{B}}T \ll \hbar\Lambda$) the lower dressed state $|\beta\rangle$ will be occupied predominantly and approaches $|0_{\text{R}}\rangle$ when the laser field is switched off [27]. Inverting the sign of the laser detuning $\hbar\Delta$ leads to the opposite process: the creation of an exciton by absorbing a photon and emitting a phonon [7, 10–13] [see blue arrow in Fig. 1(d)]. Here we note that LAPSE is fundamentally different from existing depopulation schemes, such as coherent control schemes [21, 28] and adiabatic rapid passage protocols [29–31] in which exciton-phonon coupling is usually a hindrance, whereas LAPSE is enabled by the exciton-phonon interaction.

To demonstrate the depopulation of a QD from above to below the transparency point, we first resonantly pump the QD to the exciton state at $t = 0$ using a laser pulse with pulse area $\Theta = \pi$ [see Fig. 2(a)]. Θ is defined as $(\mu_X/\hbar)\int_{-\infty}^{+\infty} E(t)\text{d}t$ and was determined from a Rabi oscillation measurement at $\hbar\Delta = 0$ meV [25, 32–34]. μ_X is the optical dipole matrix element for the $|0\rangle \to |X\rangle$ transition. The black line in Fig. 2(b) shows a PC spectrum measured as a function of the detuning of the π pulse. The peak at zero detuning corresponds to the $|0\rangle \to |X\rangle$ transition. Its amplitude PC_{π}^{X} corresponds to an exciton population of 1. Next, we apply a strong red-shifted pulse ($\hbar\Delta = -0.7$ meV, $\Theta = 5.25\pi$) to depopulate the inverted QD. In the text below, we call this red-shifted laser pulse the "LAPSE pulse". To maximize the efficiency of LAPSE, the width of the LAPSE pulse should be spectrally broad to cover as many phonon modes as possible, whereas the pulse duration τ_{L} needs to be long enough for the dressed states to complete the phonon-assisted relaxation. To fulfil both conditions, consistent with theory, we set the FWHM and τ_{L} of the LAPSE pulse to 0.42 meV and 8 ps. The red line in Fig. 2(b) shows the PC spectrum measured in the presence of the LAPSE pulse. The peak at $\hbar\Delta = -0.7$ meV is due to the interference between the π pulse and the LAPSE pulse. The reduction of the amplitude of the exciton peak PC_{2pulse}^{X} relative to PC_{π}^{X} directly demonstrates the depopulation of the exciton state. In the PC measurement, the total population of the ground state and exciton state C_{Total} drops to 0.88 at the arrival of the LAPSE pulse due to the electron tunnelling out from the QD during the delay time $\tau_{\text{delay}} = 7$ ps; therefore the

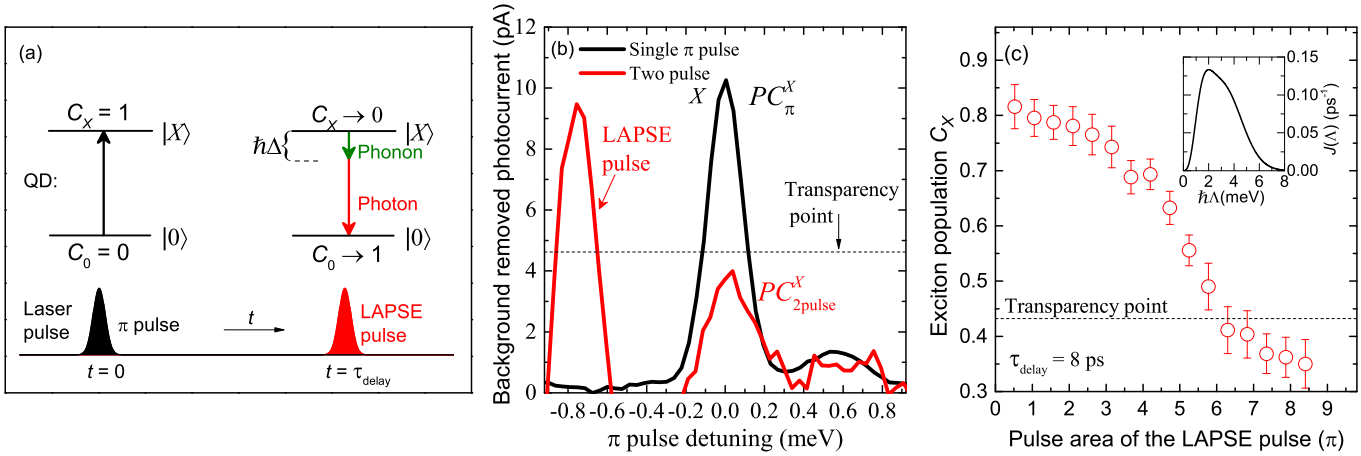

FIG. 2. (a) Scheme of the two-pulse measurement. The QD is excited to the $|X\rangle$ state by a π pulse at $t = 0$ and then depopulated by a red-shifted laser pulse (LAPSE pulse) after $\tau_{\rm delay}$. (b) Black: PC spectrum measured only with a π pulse (FWHM = 0.2 meV, $\tau_{\rm L} = 16.8$ ps). Red: Two-pulse spectrum measured in the presence of a -0.7 meV detuned LAPSE pulse (FWHM = 0.42 meV, $\tau_{\rm L} = 8$ ps, $\Theta = 5.25\pi$, $\tau_{\rm delay} = 7$ ps). PC_π^X and $PC_{\rm 2pulse}^X$ denote the amplitude of the exciton peak in the single-pulse and two-pulse spectra, respectively. The background of the PC spectra have been removed. (c) Remaining exciton population C_X after the LAPSE pulse versus the pulse area Θ. LAPSE pulse: $\hbar\Delta = -0.7$ meV, FWHM = 0.2 meV, $\tau_{\rm L} = 16.8$ ps, $\tau_{\rm delay} = 8$ ps. C_X is deduced according to: $C_X = e^{-\tau_{\rm delay}/\tau_{\rm e}} - (1 - PC_{\rm 2pulse}^X/PC_\pi^X)$, where $\tau_{\rm e}$ is the electron tunnelling time [see details in Ref. 25]. Inset: Calculated exciton-phonon coupling spectral density $J(\Lambda)$.

transparency point defined as $C_{\rm Total}/2$ is shifted to 0.44 [see details in ref. 25]. The fact that $PC_{\rm 2pulse}^X < 0.44 PC_\pi^X$ proves that the inverted QD is depopulated below the transparency point.

Fig. 2(c) shows the remaining exciton population obtained after the LAPSE pulse versus the pulse area Θ. In order to improve the spectral resolution and the signal to noise ratio, in the following measurements we reduce the FWHM of the LAPSE pulse to 0.2 meV. It can be seen that C_X decreases with the increase of Θ as predicted by the simulation in Fig. 4(b) and crosses the transparency point at $\Theta > 6.25\pi$. The minimum C_X measured here is limited by the laser power available in our setup. The efficiency of the LAPSE process strongly depends on the pulse area because the laser detuning and power determine the effective Rabi splitting $\hbar\Lambda$ that needs to be in resonance with the phonon environment for an efficient phonon-assisted relaxation to occur [35]. Fig. 2(c) inset shows the calculated exciton-phonon coupling spectral density J as a function of the effective Rabi splitting: $J(\Lambda) = \sum_{\mathbf{q}} |\gamma_{\mathbf{q}}|^2 \, \delta(\Lambda - \omega_{\mathbf{q}})$, where $\gamma_{\mathbf{q}}$ is the exciton-phonon coupling and $\mathbf{q}$ is the wave vector of bulk LA phonons [see details in Ref. 25]. Here it becomes clear that the QD can be dynamically turned from a weakly vibronic system into a strongly vibronic one by laser driving when $\hbar\Lambda$ approaches 2 meV.

We next investigate the time dynamics of LAPSE by measuring $PC_{\rm 2pulse}^X/PC_\pi^X$ versus the delay time between the π pulse and the LAPSE pulse [see red circles in Fig. 3]. At negative delay time, the LAPSE pulse arrives before the exciton is created by the π pulse and therefore cannot depopulate the exciton. The signal (~ 0.9)

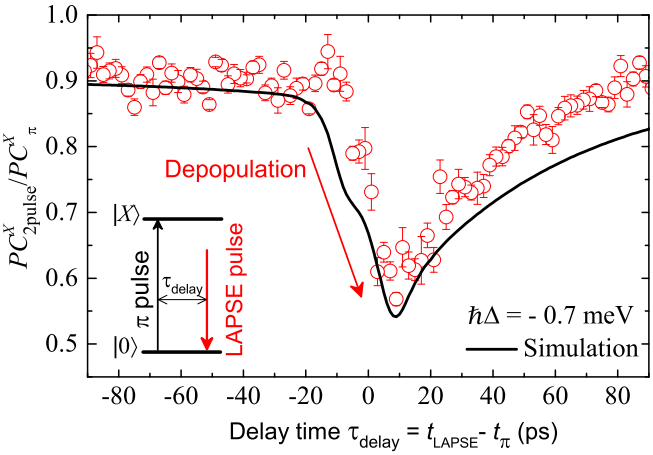

FIG. 3. Time dynamics of the LAPSE process. Red circles: $PC_{\rm 2pulse}^X/PC_\pi^X$ measured as a function of $\tau_{\rm delay}$ under the same condition as Fig. 2(c). $\tau_{\rm delay} = t_{\rm LAPSE} - t_\pi$, where $t_{\rm LAPSE}$ and t_π are the arrival times of the LAPSE pulse and the π pulse. The pulse area of the LAPSE pulse is 5.25π. Black line: Numerical simulation. Inset: Excitation scheme.

is not exactly 1 as the red-shifted LAPSE pulse can also create excitons with very small probability by absorbing phonons at $T > 0$. When the π pulse overlaps with the LAPSE pulse, $PC_{\rm 2pulse}^X$ decreases to a minimum from $\tau_{\rm delay} = -10$ to $+10$ ps, indicating that the LAPSE process can be as fast as 20 ps. The signal then slowly recovers due to the electron tunnelling before the arrival of the LAPSE pulse. The electron tunneling time (55 ps) is measured using inversion recovery techniques [24]. The

depopulation time is determined by the laser pulse width and in principle can be further reduced by using shorter laser pulses which however can diminish the efficiency of the LAPSE process when there is not enough time for the phonon-assisted relaxation to complete [10, 13]. In ref. 10 it is found that a pulse duration of about 10 ps is sufficient for the QD to reach thermal equilibrium between the two dressed states [see Fig. 1(d)].

To further verify our understanding of the time dynamics of LAPSE, we have performed path-integral calculations based on a model of a laser-driven QD coupled to LA phonons [see details in ref. 25]. The electron tunnelling occurring during the PC measurement is integrated as a Lindblad-type relaxation term into the path-integral approach without taking away the numerically complete treatment that includes all multi-phonon processes and non-Markovian effects. The calculation (black line) well reproduces all the features observed in the experiment, proving that the decrease of the PC signal is indeed caused by LAPSE.

By contrast to the fixed frequency of stimulated emission under resonant excitation, LAPSE can occur within a broad tuning range. To demonstrate this tunability, we measure the decrease of exciton population caused by a LAPSE pulse as a function of the laser detuning $\hbar\Delta$ [see Fig. 4(a)]. In this measurement, a π pulse creates a reference PC level [dashed line in Fig. 4(a)] by resonantly pumping the QD. The reference level corresponds to an exciton population of 1. Then we apply a LAPSE pulse to depopulate the exciton state and measure the PC signal as a function of the laser detuning. To isolate the signal of the QD under study from other QDs in the sample, a reference spectrum is measured with only the LAPSE pulse and subtracted [25]. The colored lines in Fig. 4(a) are the differential spectra ΔPC measured at different pulse areas. The dip at zero detuning corresponds to the resonant transition between $|X\rangle$ and $|0\rangle$. The reduction of the PC signal at negative detuning originates from the LAPSE process. The broad tuning range (~ 4 meV) is clearly demonstrated by the negative sidebands. The good agreement between the experimental result and the path-integral calculations (black lines) supports our interpretation.

Although the shape and amplitude of the sidebands shown in Fig. 4(a) are primarily determined by the spectral dependence of the exciton-phonon coupling shown in the inset in Fig. 2(c), the differential spectra ΔPC are also slightly influenced by the exciton depopulation due to electron tunnelling and the shape of the subtracted reference spectra [25]. To obtain more insight into the spectral dependence of LAPSE, we calculate the remaining exciton population obtained after the LAPSE pulse without taking into account the electron tunnelling and subtraction of the reference spectra. This simulation directly shows how the probability of LAPSE depends on the laser detuning [see Fig. 4(b)]. Furthermore the simulation for $\Theta = 7.35\pi$ clearly shows that the inverted QD is depopulated to below the transparency point at $\hbar\Delta \sim -0.7$ meV.

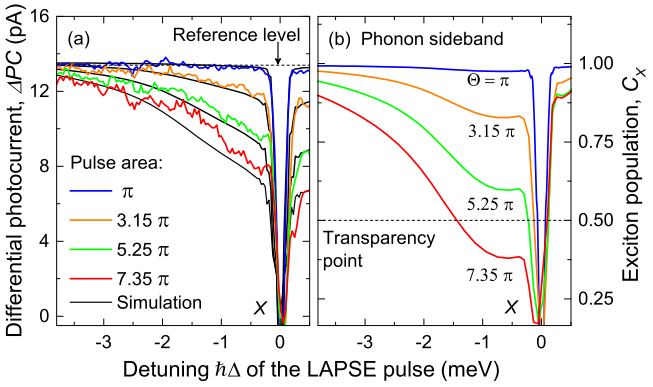

FIG. 4. Tunability of the LAPSE process. (a) Diffirential photocurrent spectra measured by pumping the QD resonantly with a π pulse and then depopulating the exciton by applying a LAPSE pulse at different detunings and pulse areas. To isolate the signal of the target QD from other QDs in the same sample, a reference spectrum where only the LAPSE pulse is applied is subtracted. $\tau_{\mathrm{delay}} = 17$ ps. Solid black lines: simulation. (b) Calculated phonon sideband without taking into account the electron tunneling and the subtraction of the reference spectra.

In conclusion, we have demonstrated the ultrafast depopulation of a QD from above to below the transparency point using red-shifted incoherent excitation via LA-phonon-assisted stimulated emission. The depopulation time ($\sim$20 ps) is determined by the laser pulse width, making it possible to reset a QD exciton much faster than the speed limitation imposed by the exciton lifetime. Due to the broadness of the phonon sideband, this scheme can occur in a tuning range of a few meV and may form the basis of tunable single QD lasers. Additionally, it can be potentially used for ultrafast optical switching [28, 36–40], semiconductor optical amplifiers [41] and precisely controlling the emission time of a single photon source in cavities [1, 16–18].

This work was funded by the EPSRC (UK) programme grant EP/J007544/1. A. M. Barth and V. M. Axt gratefully acknowledge the financial support from Deutsche Forschungsgemeinschaft via the Project No. AX 17/7-1. The authors thank A. J. Ramsay for very helpful discussions and H. Y. Liu and M. Hopkinson for sample growth.

* Email: To whom correspondence should be addressed: fengliu@sheffield.ac.uk.

[1] K. Müller, K. a. Fischer, A. Rundquist, C. Dory, K. G. Lagoudakis, T. Sarmiento, Y. a. Kelaita, V. Borish, and J. Vučković, Physical Review X **5**, 031006 (2015).

[2] K. Müller, A. Rundquist, K. a. Fischer, T. Sarmiento,

K. G. Lagoudakis, Y. a. Kelaita, C. Sánchez Muñoz, E. del Valle, F. P. Laussy, and J. Vučković, Physical Review Letters **114**, 1 (2015).
[3] A. Majumdar, A. Papageorge, E. D. Kim, M. Bajcsy, H. Kim, P. Petroff, and J. Vučković, Physical Review B **84**, 085310 (2011).
[4] A. Majumdar, M. Bajcsy, A. Rundquist, E. Kim, and J. Vučković, Physical Review B **85**, 195301 (2012).
[5] S. Weiler, A. Ulhaq, S. M. Ulrich, D. Richter, M. Jetter, P. Michler, C. Roy, and S. Hughes, Physical Review B **86**, 241304 (2012).
[6] J. R. Petta, A. C. Johnson, C. M. Marcus, M. P. Hanson, and A. C. Gossard, Physical review letters **93**, 186802 (2004).
[7] J. H. Quilter, A. J. Brash, F. Liu, M. Glässl, A. M. Barth, V. M. Axt, A. J. Ramsay, M. S. Skolnick, and A. M. Fox, Physical Review Letters **114**, 137401 (2015).
[8] T. M. Stace, A. C. Doherty, and S. D. Barrett, Physical review letters **95**, 106801 (2005).
[9] J. I. Colless, X. G. Croot, T. M. Stace, A. C. Doherty, S. D. Barrett, H. Lu, A. C. Gossard, and D. J. Reilly, Nature communications **5**, 3716 (2014).
[10] M. Glässl, A. Barth, and V. Axt, Physical Review Letters **110**, 147401 (2013).
[11] S. Hughes and H. J. Carmichael, New Journal of Physics **15**, 053039 (2013).
[12] P.-L. Ardelt, L. Hanschke, K. A. Fischer, K. Müller, A. Kleinkauf, M. Koller, A. Bechtold, T. Simmet, J. Wierzbowski, H. Riedl, G. Abstreiter, and J. J. Finley, Physical Review B **90**, 241404 (2014).
[13] S. Bounouar, M. Müller, A. M. Barth, M. Glässl, V. M. Axt, and P. Michler, Physical Review B **91**, 161302 (2015).
[14] M. Nomura, N. Kumagai, S. Iwamoto, Y. Ota, and Y. Arakawa, Nature Physics **6**, 279 (2010).
[15] E. U. Rafailov, M. A. Cataluna, and W. Sibbett, Nature Photonics **1**, 395 (2007).
[16] D. Heinze, D. Breddermann, A. Zrenner, and S. Schumacher, Nature communications **6**, 8473 (2015).
[17] C. S. Muñoz, F. P. Laussy, C. Tejedor, and E. del Valle, ArXivxiv (2015), arXiv:1506.05050.
[18] S. L. Portalupi, G. Hornecker, V. Giesz, T. Grange, A. Lemaître, J. Demory, I. Sagnes, N. D. Lanzillotti-Kimura, L. Lanco, A. Auffèves, and P. Senellart, Nano letters **15**, 6290 (2015).
[19] J. Klein and J. D. Kafka, Nature Photonics **4**, 289 (2010).
[20] A. Vagov, M. D. Croitoru, M. Glässl, V. M. Axt, and T. Kuhn, Physical Review B **83**, 094303 (2011).
[21] A. Zrenner, E. Beham, S. Stufler, F. Findeis, M. Bichler, and G. Abstreiter, Nature **418**, 612 (2002).
[22] A. J. Brash, L. M. P. P. Martins, F. Liu, J. H. Quilter, A. J. Ramsay, M. S. Skolnick, and A. M. Fox, Physical Review B **92**, 121301 (2015).
[23] T. M. Godden, J. H. Quilter, A. J. Ramsay, Y. Wu, P. Brereton, I. J. Luxmoore, J. Puebla, A. M. Fox, and M. S. Skolnick, Physical Review B **85**, 155310 (2012).
[24] R. S. Kolodka, A. J. Ramsay, J. Skiba-Szymanska, P. W. Fry, H. Y. Liu, A. M. Fox, and M. S. Skolnick, Physical Review B **75**, 193306 (2007).
[25] See Supplementary Material at [url] for the description of the model and the derivation of the exciton population, which includes refs. [7, 20, and 26].
[26] H.-P. Breuer and F. Petruccione, *The Theory of Open Quantum Systems* (Oxford University Press, USA, 2002).
[27] A. M. Barth, S. Lüker, A. Vagov, D. E. Reiter, T. Kuhn, and V. M. Axt, (2016), arXiv:1601.07886.
[28] A. Heberle, J. Baumberg, and K. Köhler, Physical Review Letters **75**, 2598 (1995).
[29] Y.-J. Wei, Y.-M. He, M.-C. Chen, Y.-N. Hu, Y. He, D. Wu, C. Schneider, M. Kamp, S. Höfling, C.-Y. Lu, and J.-W. Pan, Nano letters **14**, 6515 (2014).
[30] R. Mathew, E. Dilcher, A. Gamouras, A. Ramachandran, H. Y. S. Yang, S. Freisem, D. Deppe, and K. C. Hall, Physical Review B **90**, 035316 (2014).
[31] S. Lüker, K. Gawarecki, D. E. Reiter, A. Grodecka-Grad, V. M. Axt, P. Machnikowski, and T. Kuhn, Physical Review B **85**, 121302 (2012).
[32] A. J. Ramsay, T. M. Godden, S. J. Boyle, E. M. Gauger, A. Nazir, B. W. Lovett, A. M. Fox, and M. S. Skolnick, Physical Review Letters **105**, 177402 (2010).
[33] A. J. Ramsay, A. V. Gopal, E. M. Gauger, A. Nazir, B. W. Lovett, A. M. Fox, and M. S. Skolnick, Physical Review Letters **104**, 017402 (2010).
[34] L. Monniello, C. Tonin, R. Hostein, A. Lemaitre, A. Martinez, V. Voliotis, and R. Grousson, Physical Review Letters **111**, 026403 (2013).
[35] A. Nazir, Physical Review B **78**, 153309 (2008).
[36] N. H. Bonadeo, Science **282**, 1473 (1998).
[37] R. Bose, D. Sridharan, H. Kim, G. S. Solomon, and E. Waks, Physical Review Letters **108**, 227402 (2012).
[38] T. Volz, A. Reinhard, M. Winger, A. Badolato, K. J. Hennessy, E. L. Hu, and A. Imamolu, Nature Photonics **6**, 607 (2012).
[39] D. Englund, A. Majumdar, M. Bajcsy, A. Faraon, P. Petroff, and J. Vučković, Physical Review Letters **108**, 2 (2012), arXiv:1107.2956.
[40] E. Cancellieri, A. Hayat, A. M. Steinberg, E. Giacobino, and A. Bramati, Physical Review Letters **112**, 053601 (2014).
[41] A. Capua, O. Karni, G. Eisenstein, V. Sichkovskyi, V. Ivanov, and J. P. Reithmaier, Nature Communications **5**, 5025 (2014).